Biochemical Pharmacology 77 (2009) 1383–1390

Contents lists available at ScienceDirect

Biochemical Pharmacology

journal homepage: www.elsevier.com/locate/biochempharm

Electrophysiologic characterization of a novel hERG channel activator

Zhi Su [a,*], James Limberis [a], Andrew Souers [b], Philip Kym [c], Ann Mikhail [a], Kathryn Houseman [a], Gilbert Diaz [a], Xiaoqin Liu [a], Ruth L. Martin [a], Bryan F. Cox [a], Gary A. Gintant [a]

[a] Department of Integrative Pharmacology, Abbott Laboratories, R46R-AP9, 100 Abbott Park Road, Abbott Park, IL 60064, USA
[b] Cancer Research, Abbott Laboratories, 100 Abbott Park Road, Abbott Park, IL 60064, USA
[c] Neuroscience Research, Abbott Laboratories, 100 Abbott Park Road, Abbott Park, IL 60064, USA

ARTICLE INFO

Article history:
Received 3 December 2008
Accepted 22 January 2009

Keywords:
hERG activator
K-channel
Action potential
A-935142

ABSTRACT

Activators of the human ether-a-go-go-related gene (hERG) K^+ channel have been reported recently to enhance hERG current amplitude (five synthetic small molecules and one naturally occurring substance). Here, we characterize the effects of a novel compound A-935142 ({4-[4-(5-trifluoromethyl-1H-pyrazol-3-yl)-phenyl]-cyclohexyl}-acetic acid) on guinea-pig atrial and canine ventricular action potentials (microelectrode techniques) and hERG channels expressed in HEK-293 cells (whole-cell patch clamp techniques). A-935142 shortened cardiac action potentials and enhanced the amplitude of the hERG current in a concentration- and voltage-dependent manner. The fully activated current–voltage relationship revealed that this compound (60 μM) increased both outward and inward K^+ current as well as the slope conductance of the linear portion of the fully activated *I–V* relation. A-935142 significantly reduced the time constants (τ) of hERG channel activation at two example voltages (−10 mV: τ = 100 ± 17 ms vs. 164 ± 24 ms, $n = 6$, $P < 0.01$; +30 mV: τ = 16.7 ± 1.8 ms vs. 18.9 ± 1.8 ms, $n = 5$, $P < 0.05$) and shifted the voltage-dependence for hERG activation in the hyperpolarizing direction by 9 mV. The time course of hERG channel deactivation was slowed at multiple potentials (−120 to −70 mV). A-935142 also reduced the rate of inactivation and shifted the voltage-dependence of inactivation in the depolarizing direction by 15 mV. Recovery of hERG channel from inactivation was not affected by A-935142. In conclusion, A-935142 enhances hERG current in a complex manner by facilitation of activation, reduction of inactivation, and slowing of deactivation, and abbreviates atrial and ventricular repolarization.

1. Introduction

The human ether-a-go-go-related gene (hERG or KCNH2) encodes the α subunits of a rapidly activating delayed inward rectifier channel (Kv11.1), which conducts an essential repolarization potassium current (I_{Kr}) during cardiac action potential [1–3]. Genetic defects or drug block of the I_{kr} channel causes delayed repolarization of cardiac action potentials, which is manifested as prolongation of QT interval on the body surface electrocardiography [3,4]. The delayed repolarization predisposes patients to ventricular tachycardia and Torsades de Pointes (Tdp), which may degenerate into ventricular fibrillation. A constellation of cardiac abnormalities caused by the delayed repolarization is referred to as long QT syndromes (LQTS) [4,5].

Because of the rare (but severe) consequences of drug-induced delayed repolarization, novel drug candidates are routinely screened for hERG current block that is seen with diverse chemical structures from different therapeutic areas [6–8]. These enhanced screening efforts have resulted in recent reports of compounds that enhance hERG current [9–17]. The five compounds described reportedly increase hERG current by different mechanisms. RPR260243 induces two distinct changes in hERG gating: a slowing of deactivation and a positive shift in the voltage-dependence of inactivation [9,15], while NS1643 and NS3623 enhance hERG current magnitude by reducing channel inactivation [11–13,17]. The mechanism of action of PD-118057 is still unknown [10]. In contrast, PD-307243, a structure analog of PD-118057, increased hERG current with the rates of both inactivation and deactivation being slowed markedly [16].

In a recent hERG screen, we identified A-935142 as a compound with significant hERG-enhancing activity. In this study we demonstrated the ability of A-935142 to shorten repolarization of guinea-pig atrial and canine Purkinje fiber action potentials, as well as characterized its effects on hERG current heterologously expressed in HEK-293 cells. Specifically we showed that A-935142 induced a complex set of changes in hERG channel gating, including facilitation of activation, reduction of inactivation, and slowing of deactivation. Furthermore, we also found that A-935142 increased the slope

* Corresponding author. Tel.: +1 847 935 4784; fax: +1 847 938 5286.
E-mail address: zhi.su@abbott.com (Z. Su).

0006-2952/$ – see front matter © 2009 Elsevier Inc. All rights reserved.
doi:10.1016/j.bcp.2009.01.015

conductance of the linear portion of the fully activated *I–V* relation, a novel mechanism of action not consistently described for the previously reported hERG activators. These studies highlight the diversity of biophysical effects possible with hERG channel activators.

2. Methods and materials

2.1. Culture of HEK-293 cells

The stable transfection of HEK-293 cells with wild-type (WT) hERG cDNA (hERG1 or KCNH2) has been previously described [18]. Transfected HEK-293 cells were maintained at 37 °C in Minimal Eagle Medium (MEM) supplemented with 10% fetal bovine serum, 1% penicillin–streptomycin, 2 mM L-glutamine, 0.1 mM nonessential amino acids, 1 mM sodium pyruvate, and 0.2 mg/ml geneticin (Invitrogen Corporation, Carlsbad, CA, USA). Cells were passaged weekly and were not allowed to become more than 80% confluent. For electrophysiological recordings, the cells were harvested from the culture dish by trypsinization, washed twice with standard MEM, and maintained in culture medium at room temperature for later use on the same day [19].

2.2. Electrophysiology

HERG potassium current in HEK-293 cells was recorded at 37 °C using a whole-cell patch clamp technique (Axopatch 200A amplifier). Cells were voltage-clamped with single suction pipettes (initial resistances of 1.2–2.6 MΩ) made from borosilicate glass capillary tubing. Series resistance compensation (75–80%) was used in all experiments. Currents were filtered at 2–5 kHz and digitized at 5–10 kHz. The pClamp 8 software (Axon Instruments, Sunnyvale, CA) was used to generate voltage clamp protocols and acquire data [19].

Action potentials from guinea-pig atrial tissues and canine cardiac Purkinje fibers were recorded using a conventional microelectrode technique [20]. Briefly, left atrial tissues from guinea-pig heart or free-running Purkinje fibers from either ventricle of canine heart were harvested and placed in a warmed chamber (37 °C), which was superfused with Tyrode's solution (8–10 ml/min). Atrial tissues or Purkinje fibers were stimulated (2× threshold, biphasic waveform, typically 1–2 ms in duration) using platinum electrodes located in the chamber floor and impaled with 3 M KCl-filled microelectrodes (resistance 10–30 MΩ). Electrical activity was monitored using high-input impedance electrometers (IE-210, Warner Instruments, Hamden CT). Studies were initiated after a minimum of 30 min equilibration with stimulation.

2.3. Solutions and drugs

For voltage clamp experiments, HEK-293 cells were superfused with a HEPES-buffered Tyrode's solution containing (in mM): 140 NaCl, 5 KCl, 1 $MgCl_2$, 2 $CaCl_2$, 5 glucose, 20 HEPES (pH 7.4, adjusted with NaOH). The pipette solution for HEK-293 cells contained (in mM): 125 K aspartate, 20 KCl, 10 EGTA, 1 $MgCl_2$, 5 MgATP, 5 HEPES (pH 7.3, adjusted with KOH) [19]. For action potential recording, Purkinje fibers or guinea-pig atrial preparations were superfused with Tyrode's solution containing (in mM)): 131 NaCl, 18 $NaHCO_3$, 1.8 NaH_2PO_4, 0.5 $MgCl_2$, 5.5 glucose, 4 KCl, 2 $CaCl_2$ (aerated with 95% O_2/5% CO_2) [20]. A-935142 ({4-[4-(5-trifluoromethyl-1H-pyrazol-3-yl)-phenyl]-cyclohexyl}-acetic acid) was synthesized by Abbott Laboratories (Abbott Park, IL), prepared as a stock solution in DMSO and then diluted as desired with Tyrode's solution or HEPES-buffered Tyrode's solution. The maximum DMSO concentration in the final perfusate was less than 0.1%. A-935142 (for each concentration) was applied for 5 min in studies with HEK-293 cells and for 20 min in studies with tissue preparations. DMSO, aspartate (K^+ salt), and HEPES were purchased from Sigma–Aldrich (St. Louis, MO). All other chemicals were obtained from Fisher Scientific (Fair Lawn, NJ)

2.4. Data analysis

Recordings were digitized online with a DigiData 1200 interface (Axon Instruments, Inc.) and stored on a computer hard disk or a local-area network drive. The digitized data were analyzed with pClamp8 (Axon Instruments, Inc.) and ORIGIN software (Origin Lab Corporation, Northampton, MA, USA). Results were expressed as means ± S.E.M. Statistical differences were evaluated by unpaired or paired *t*-tests and were considered significant at $P < 0.05$.

3. Results

3.1. Effects of A-935142 on hERG current and action potential duration

A-935142 was found to increase hERG K^+ current in a concentration-dependent manner. As shown in panel B of Fig. 1, hERG current was elicited by a ramp protocol (1 s step to +20 mV from a holding potential of −80 mV, followed by a 2-s ramp back to the holding potential). A-935142 increased both activation and tail current amplitudes. The activation current amplitude measured at the end of the 1-s depolarization pulse and the peak tail current amplitude during repolarization were increased by 59% and 47%, respectively, in the presence of 60 μM A-935142. Similar increases in current were also seen in experiments using a different ramp protocol in which we employed a 1-s step to 0 mV followed by a 2-s ramp (56% increase for activation current, 43% for peak tail current). It should be noted that higher concentrations of A-935142 were not tested due to limited aqueous solubility in the HEPES-buffered Tyrode's solution. Therefore, a full concentration–response curve (or an EC_{50} value) was not obtained for the effects of A-935142 on hERG current.

Because of the importance of hERG current (I_{kr} in native tissue) in repolarization of the cardiac action potential, the hERG-enhancing effect by A-935142 suggests its ability to shorten the action potential duration of native cardiac tissue. To test this possibility, we recorded action potentials in canine cardiac Purkinje fibers and guinea-pig left atria using conventional microelectrode technique [20]. As illustrated in panel C of Fig. 1, the action potential duration of the Purkinje fiber at 50% repolarization (APD50) or 90% repolarization (APD90) was decreased in a concentration-dependent manner, with APD90 reduced by 23.5 ± 1.7% ($n = 4$, $P < 0.01$) and APD50 by 22.1 ± 4.9% ($P < 0.05$) in the presence of 60 μM A-935142. However, A-935142 had little effects on the maximal upstroke velocity (control vs. drug (60 μM): 585 ± 35 V/s vs. 535 ± 32 V/s, $P > 0.05$) and resting membrane potential (control vs. drug: 92.1 ± 0.6 mV vs. 92.6 ± 0.8 mV, $P > 0.05$) of the dog Purkinje fiber action potential. The action potential duration of guinea-pig atria was also significantly decreased in the presence of 60 μM A-935142 (panel D in Fig. 1), with APD90 decreased by 18 ± 3.9% ($n = 4$, $P < 0.01$) and APD50 by 11.2 ± 2.2% ($P < 0.05$). Resting membrane potential in guinea-pig atria was not altered by A-935142 at 60 μM (control vs. drug: 86.7 ± 2.7 mV vs. 87.4 ± 2.7 mV, $P > 0.05$). These results indicate that I_{Kr} in native cardiac tissue is activated by A-935142, resulting in a shortening of the action potential duration. Lack of effects on other action potential parameters (such as amplitude, upstroke velocity, plateau amplitude, and resting membrane potential) suggests that A-935142 may not have any significant effects on other ion channels involved in the action potential at concentrations up to 60 μM.

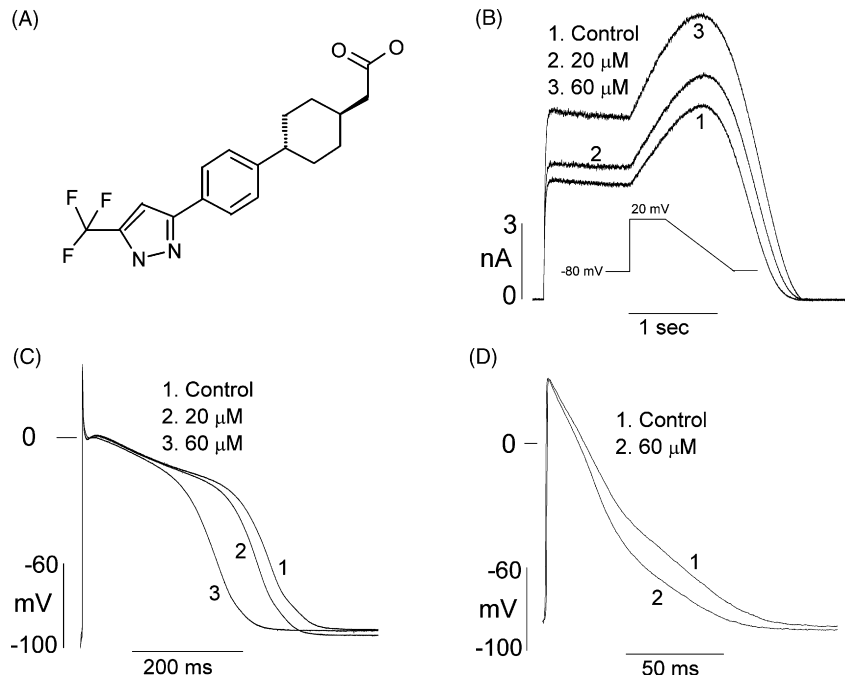

Fig. 1. A-935142 enhances hERG current and shortens action potential duration. Panel A: structure of A-935142. Panel B: effects of A-935142 on hERG current elicited by a 1-s step to 20 mV followed by a 2-s ramp to −80 mV. The voltage protocol (see inset) was applied every 10 s with a holding potential of −80 mV for 5 min. Panels C and D: representative effects of A-935142 on action potential duration of a canine Purkinje fiber (panel C) and guinea-pig left atria (panel D). Action potentials (in panels C and D) were recorded using standard microelectrode techniques and slow stimulation (0.5 Hz).

3.2. Effect of A-935142 on hERG channel activation

To further understand the mechanisms responsible for enhancement of hERG current with A-935142, we first evaluated its effect on the voltage-dependence of hERG activation. Using the protocol shown in Fig. 2, hERG current was activated in the absence (control, Fig. 2A) and presence of 60 μM A-935142 (Fig. 2B). Activation (I_{act}, Fig. 2C) and tail current amplitudes (I_{tail}, Fig. 2D) were significantly enhanced at test potentials positive to −60 mV. The current–voltage plot for peak tail current (activation curve) was fitted to a Boltzmann function. The half maximal activation voltage ($V_{1/2}$) was shifted leftward (−39.9 ± 1.6 mV vs. −30.6 ± 0.9 mV, $P < 0.05$, $n = 6$) and the slope factor was unchanged. Further analysis revealed that hERG current enhancement by A-935142 is steeply voltage-dependent in the

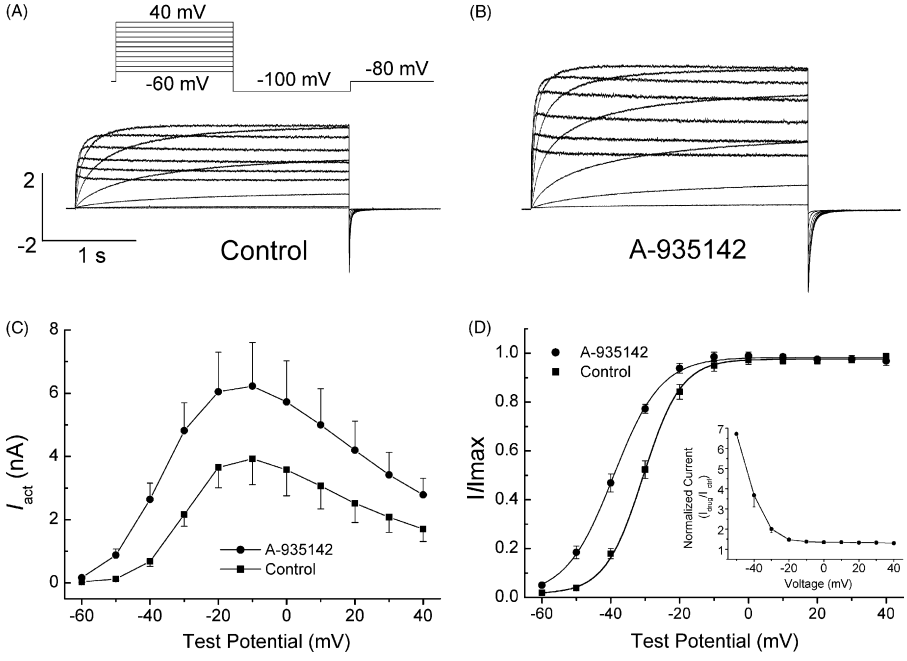

Fig. 2. Voltage-dependent increase of hERG current by A-935142. Panels A and B: currents recorded in the absence (panel A) and presence (panel B) of A-935142 (60 μM). Drug exposure time was 5 min. Voltage protocol shown in inset. Panel C: current–voltage plot for activating current measured at the end of depolarizing voltage steps. Panel D: the plot of normalized tail current amplitude vs. test potentials was fitted to a Boltzmann equation to obtain the half-point ($V_{1/2}$) and slope factor (k) for channel activation: $I/I_{max} = 1/(1 + \exp[(V_{1/2} - V)/k])$. The voltage-dependence of hERG activation is shifted by A-935142 (control, $V_{1/2} = -30.6 \pm 0.9$ mV; A-935142, $V_{1/2} = -39.9 \pm 1.6$ mV; the slope factor was unchanged). Inset demonstrates steep voltage-dependence for hERG current enhancement over the voltage range of −50 to −20 mV. Normalized current is the ratio of current amplitudes in the presence (I_{drug}) and absence (I_{ctrl}) of A-935142. Data were expressed at mean ± S.E.M. ($n = 6$).

range of −50 to −20 mV (inset in Fig. 2D), consistent with a leftward shift in the voltage-dependence of activation.

The effect of A-935142 on the activation kinetics of hERG current was assessed using an envelope of tails test [21,22]. Cells were held at −80 mV and pulsed to −10 mV for selected durations (5–850 ms, 30 ms increment, Fig. 3A and B). Tail currents recorded at −100 mV were plotted against the activation pulse duration to construct the activation time course, which was fitted with a single exponential function (Fig. 3C). A-935142 at 60 μM significantly reduced the activation time constant of hERG current at −10 mV (100 ± 17 ms vs. 164 ± 24 ms, $n = 6$, $P < 0.01$), indicating acceleration of hERG activation, consistent with a hyperpolarizing shift in the voltage-dependence of hERG activation. The activation time course of hERG current at +30 mV was also accelerated by A-935142 (data not shown).

3.3. Effect of A-935142 on hERG channel deactivation

The deactivation kinetics of hERG current were examined in the voltage range of −70 to −120 mV using a protocol shown in Fig. 4A. The time course of the deactivating tail currents was fitted with a double exponential function to obtain the fast and slow time constants. To facilitate visual comparison in tail current kinetics between control and treatment, scaled tail currents were displayed in panels C and D for two representative test voltages (−70 and −120 mV). The time course of the deactivating tail currents at multiple voltages is markedly slowed by A-935142 (Fig. 4A–D), i.e. increased time constants in both fast (Fig. 4E) and slow (Fig. 4F) components. The slowed deactivation in the presence of A-935142 suggests that delayed closure of the activation gate contributes to the enhanced hERG current.

3.4. Effect of A-935142 on hERG channel inactivation and recovery from inactivation

A three-pulse protocol (Fig. 5A) was used to assess the onset rate of the hERG current inactivation. Following a 500-ms pulse to +60 mV (to allow the current to fully activate and inactivate), a 2-ms pulse was applied to −100 mV to remove inactivation. A test pulse (the third pulse in the protocol) to potentials ranging from −40 to +60 mV was then applied to induce the re-onset of channel inactivation. Time constants of inactivation were determined by a single exponential fitting of the inactivating currents elicited during the test pulse (Fig. 5A and B). As shown in Fig. 5C, the inactivation time constants were significantly increased by A-935142 at voltages more positive than −40 mV, indicating the onset rate of hERG channel inactivation was significantly reduced. The relative increase in time constants (calculated as the ratio of τ values measured in the presence and absence of A-935142) was voltage-dependent (inset, Fig. 5C).

Rapid C-type inactivation reduces hERG current magnitude at positive potentials and causes inward rectification of the fully activated *I–V* relationship [23,24]. Because A-935142 significantly reduced the onset rate of hERG current inactivation and this effect was voltage-dependent, we next examined the effect of A-935142 on the voltage-dependence of steady-state inactivation by comparing the half-point ($V_{1/2}$) of the rectification–voltage relationship [12,15]. The fully activated *I–V* relationship for hERG was determined using a protocol in Fig. 6A, in which we measured the peak amplitude of tail currents over a wide range of membrane potentials after a 1-s pulse to +40 mV. As shown in Fig. 6C, the reversal potential was not changed by A-935142. A-935142 increased tail current amplitudes at test voltages positive to the reversal potential, reducing the rectification of hERG current. This effect was quantified by measuring the rectification factor, defined as the deviation (reduction) of current amplitudes relative to that obtained from the extrapolation of the linear portion of the *I–V* relationship (between −120 and −90 mV) to more positive potentials. A-935142 at 60 μM shifted the $V_{1/2}$ of the rectification–voltage relationship by 15 mV (Fig. 6D, $n = 7$). Thus, increased hERG current with A-935142 is, at least in part, due to a decrease in the extent of hERG channel inactivation.

It is interesting to note that A-935142 also increased the tail current amplitude at test voltages negative to the reversal potential, resulting in an increase in the slope conductance of the linear portion of the fully activated *I–V* relationship (389 ± 46 nS vs. 368 ± 44 nS, $n = 5$, $P < 0.05$). This effect on the slope conductance suggests that A-935142 may increase the single-channel conductance of hERG channel.

We also analyzed the time course of recovery from inactivation by applying a monoexponential fitting of the ascending phase of tail currents from Fig. 6A and B in the absence and presence of

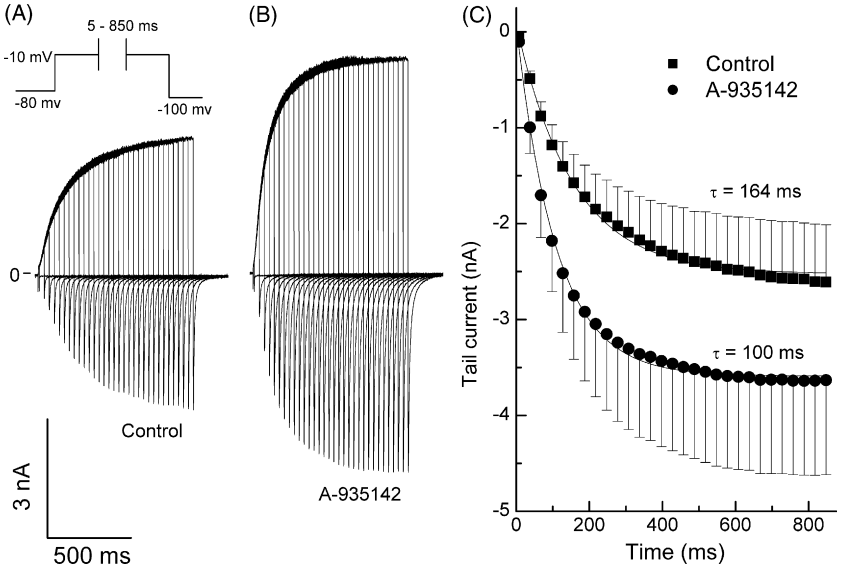

Fig. 3. A-935142 accelerates hERG activation kinetics. Panels A and B, activation time course of hERG current (at −10 mV) assessed before (panel A, control) and after exposure to 60 μM A-935142 for 5 min (panel B) using an envelope of tails test (protocol is shown above the current traces). Panel C, pooled data ($n = 5$) for the activation time course. A-935142 accelerated hERG activation (control $\tau = 164$ ms, A-935142 $\tau = 100$ ms).

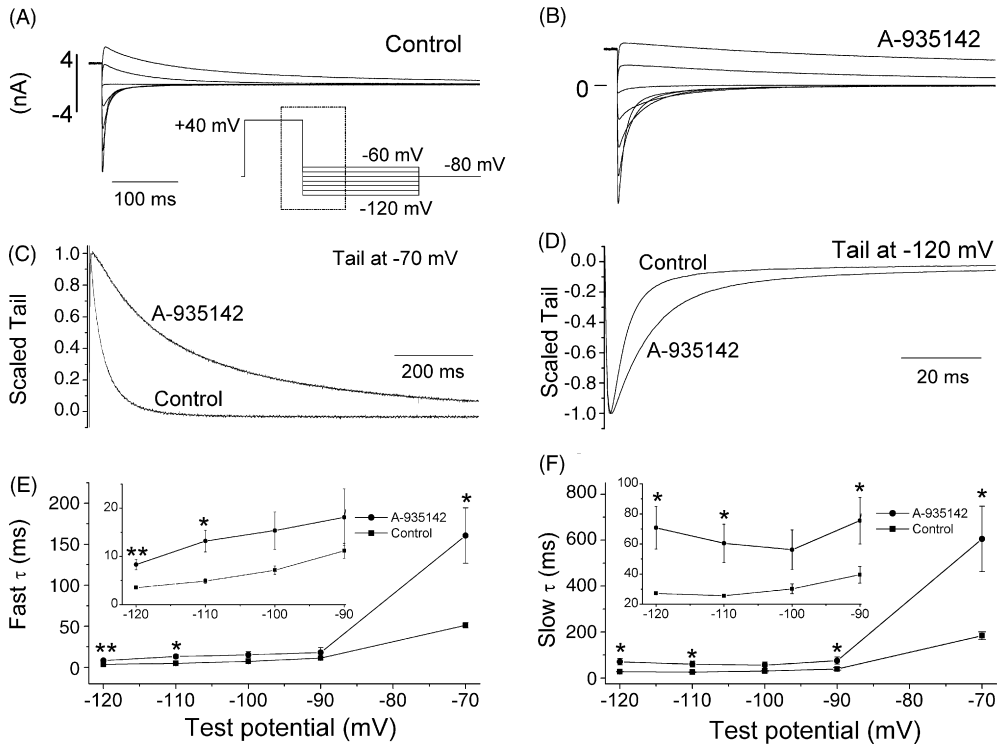

Fig. 4. A-935142 slows hERG deactivation kinetics. Panels A and B, tail currents recorded using the voltage protocol illustrated below the current traces in panel A. Currents were obtained from the same cell before (control) and after treatment with A-935142 (60 μM) for 5 min. Currents during the protocol segment highlighted by dashed lines are shown. Panels C and D: comparison of scaled tail currents recorded at −70 mV (panel C) and −120 mV (panel D) before (control) and after treatment with A-935142. Panels E and F: time constants (τ) for fast and slow components of current deactivation in the absence (control) and presence of A-935142 (60 μM). Data were expressed as mean ± S.E.M. (n = 7). Insets in panels E and F are expanded plots (with reduced y-axis scales) to show the differences in τ values between control and A-935142 at low voltages (−120 to −90 mV).

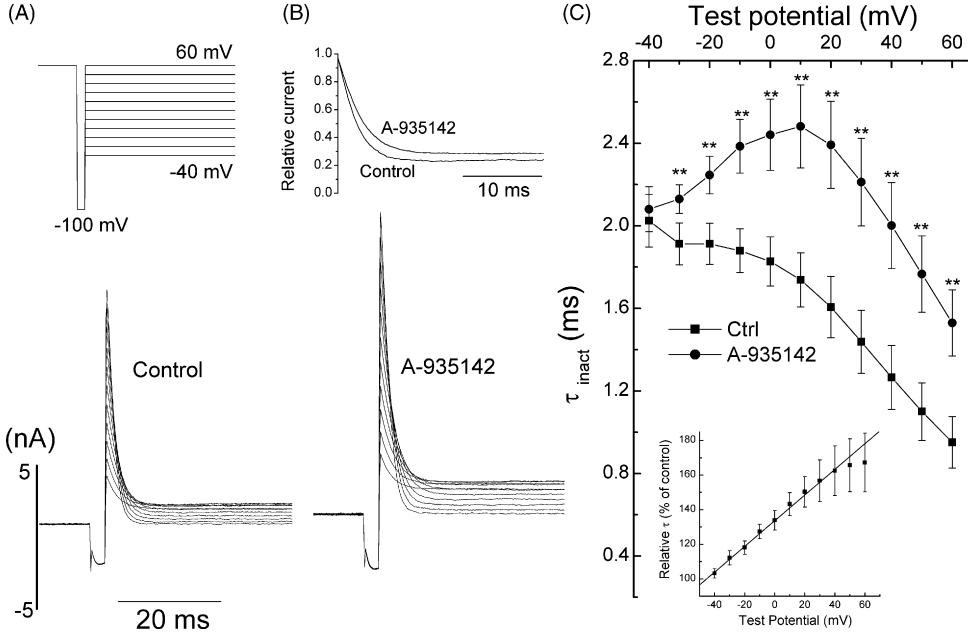

Fig. 5. A-935142 slows hERG inactivation kinetics. Panels A and B: representative traces showing the effect of A-935142 on the inactivating rate of hERG currents. A three-pulse protocol (as initially described by Smith et al. [23] and Spector et al. [24], see panel A) was used to assess the onset of inactivation. Inset in panel B: comparison of scaled inactivation time course (at 0 mV) in the absence (control) and presence of A-935142 (for 5 min), with fit time constants of 1.7 ms (control) and 2.6 ms (A-935142). Panel C: inactivation time constant plotted as a function of test voltages. Time constants were determined by fitting the inactivating currents (panels A and B) to a single exponential function. At voltages equal or positive to −30 mV, the time constants were significantly increased by A-935142 (**$P < 0.01$). The slowing of hERG inactivation was voltage-dependent (inset in panel C). The relative increase was calculated as the ratio of the τ values measured in the presence and absence of A-935142. Data expressed as mean ± S.E.M. (n = 6). [A-935142] = 60 μM.

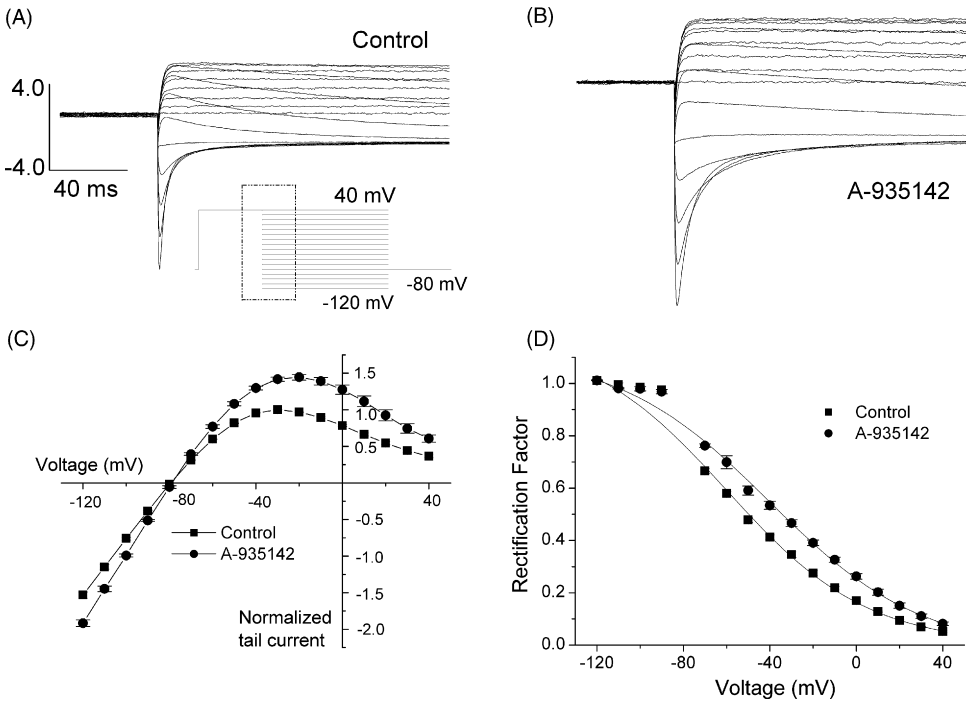

Fig. 6. Effects of A-935142 on rectification of hERG channel. Representative hERG currents recorded before (panel A, control) and after exposure (panel B) to A-935142 (60 μM) for 5 min. Voltage clamp protocol used to examine the fully activated *I–V* relationship of hERG is shown below the current traces in panel A. Current in the protocol segment highlighted by the dashed line is shown in panels A and B. Panel C: fully activated *I–V* relationship. Currents were normalized to the peak of the outward control current in the absence of compound. Currents in the presence of compound were normalized to their matched controls. Panel D: voltage-dependence of inactivation determined from rectification of the fully activated *I–V* relationship. The inactivation curve was fitted with a Boltzmman function. $V_{1/2}$ was -51.6 ± 2.3 mV for control, -35.4 ± 2.2 mV for A-935142 at 60 μM. The slope factor was not changed (control, 32.6 ± 1.9 mV; A-935142, 35.0 ± 1.7 mV). Data were expressed as mean ± S.E.M. ($n = 7$). Some error bars in panels C and D are encompassed in the symbols.

A-935142. Although the onset rate and extent of hERG channel inactivation are reduced by A-935142, recovery from inactivation was not significantly altered.

4. Discussion

The present study demonstrates multiple and complex effects of A-935142 on hERG current. Specifically, A-935142 induced three distinct changes in hERG channel gating: (a) facilitating activation (a negative shift of the voltage-dependence of activation and accelerated activation kinetics), (b) a slowing of deactivation, and (c) reduction of inactivation (a positive shift of the voltage-dependence of inactivation and reduced onset of inactivation). At present, only six hERG activators have been studied in detail, these studies have demonstrated less complex mechanisms by which compounds enhance hERG current. Both RPR260243 and PD-307243 increase hERG current by slowing deactivation and reducing inactivation [9,15,16]. PD-118057 may only reduce channel inactivation [10]. NS1643 was initially reported to enhance hERG current magnitude without measurable effects on current kinetics [11]. Later on, NS1643 was shown to reduce inactivation and slow deactivation of the hERG channel [12,17]. NS3623 enhances hERG current magnitude by reducing channel inactivation with little or no effect on the rate of deactivation [13]. Mallotoxin is a naturally occurring substance, which increases hERG current magnitude by accelerating activation and slowing deactivation [14]. None of the previously reported small molecule activators has shown consistent effects on the voltage-dependence of hERG channel activation. Xu et al. described a hyperpolarizing shift in the voltage-dependence of hERG activation in oocytes in response to NS1643 at 30 μM [17]. However, this effect was not observed in the previous study using the same hERG expression system at the same concentration [12]. Similar to previously reported activators, A-935142 significantly increased outward hERG current (including step and tail current) (Figs. 1, 2 and 6). Interestingly, A-935142 also increased the inward tail current (Figs. 2, 4 and 6), as evidenced by an increase in the slope conductance of the linear portion of the fully activated *I–V* relationship (Fig. 6C). This effect may represent a novel mechanism for hERG current enhancement. NS1643 was the only reported activator that was shown to increase hERG tail current at negative potentials from a fully activated *I–V* study at 30 μM in oocytes [17]. However, this effect was not observed in a previous study using oocytes at concentrations up to 30 μM [12]. It is not clear why there were differences between the two studies with NS 1643 in terms of the effects on the voltage-dependence of hERG activation and the inward tail at voltages negative to the reversal potentials [12,17]; it is possible that different lots or batches of NS 1643 were used in the two studies. Finally, it is also interesting to note that none of the reported hERG activators (including A-935142) demonstrate any significant effects on the rate of recovery from inactivation of hERG channel. Overall, hERG activators with different structures exhibit different profiles on the gating properties of the heterologously expressed hERG channel. Detailed studies of more hERG activators are required to help us gain insightful information on their structure–activity relationships.

The major pathogenesis of LQTS is the delayed cardiac repolarization (i.e. action potential duration prolongation, which is manifested as QT interval prolongation on body surface ECG) that can be caused by multiple channelopathies such as negative-dominant mutation in hERG channel and drug-induced inhibition of hERG channel [4,5,7]. The major pharmacological outcome of hERG activators is acceleration of the cardiac repolarization (action potential duration shortening) as reported previously [10,11] and in this study. Therefore, it has been proposed that selective enhancement of hERG channel activity could be a novel

antiarrhythmic approach, particularly as an alternative and specific treatment for inherited or acquired LQTS [10–12,15,25,26]. However, this concept has yet to be proven preclinically or clinically. Zhou et al. have shown that "early afterdepolarizations (EADs)" induced by dofetilide were completely eliminated by the hERG activator PD-118057 in an arterially perfused rabbit ventricular wedge preparation [10]. Very recently, Killeen et al. reported that NS1643 significantly reduced LQTS-type arrhythmias induced by hypokalaemia in the isolated murine hearts [27].

In contrast to its potential therapeutic application, hERG activation could be an unwanted off-target effect of drugs developed for non-cardiovascular indications. Unintended enhancement of hERG channel activity could pose a risk of acquired short QT syndrome (SQTS). It is now considered important to accurately gauge whether a QT interval is too long or excessively shortened, as the patient is at risk for sudden cardiac death from either QT syndrome [28,29]. At present, it is uncertain if the risk of ventricular proarrhythmia is equal for comparable QT prolongation and QT shortening. It should be noted that atrial fibrillation is also observed in SQTS in addition to ventricular fibrillation. This is probably because atrial fibrillation is associated with shortening of APD and effective refractory period [30]. However, given the lack of reported documentation of drug-induced SQTS in both animal models and clinical scenarios, the potential safety liability associated with hERG activation remains to be determined. Recently, Itoh et al. have proposed that arrhythmogenesis might be associated not only with gain of function (hERG current enhancement), but also with accelerated deactivation of hERG channel. This proposal was formulated through a simulation study based on the electrophysiological properties of a mutant hERG channel (N588K) that produced a short QT-syndrome [31,32]. In contrast, most hERG channel activators including A-935142 have been shown to slow the deactivation kinetics. In addition, N588K mutant has an extreme right-ward shift of the inactivation curve of more than 100 mV that is never observed with the reported hERG channel activators. Therefore, in addition to current enhancement (through gain-of-function mutation or hERG agonists), it is possible that unique changes in the gating properties of hERG channel are linked to arrhythmogenesis in short QT syndrome.

Although the clinical fate of specific hERG activators as an antiarrhythmic approach and the safety concern of unintended hERG activation are uncertain, understanding the molecular mechanisms responsible for hERG channel activation is as important as that for hERG channel blockers. Two groups have recently taken the lead in exploring the mechanisms of hERG activators on a molecular level [12,15,17]. Casis et al. have shown that NS1643 did not enhance hERG current magnitudes in three inactivation-deficient hERG mutant channels (S620T, S631A, and G628C/S631C), indicating that reduced channel inactivation is the major mechanism of action for the agonist effect of NS1643 on hERG channel [12,17]. Furthermore, Xu et al. have provided interesting evidence showing that NS1643 acts on the hERG channel from the extracellular site of the cell membrane possibly by binding to outer vestibule/pore entrance of hERG [17]. However, it remains to be understood how the binding of NS1643 to the outer vestibule and pore entrance of hERG is associated with the reduced inactivation [17]. In contrast, it has been found that RPR260243 interacts with a cluster of residues (L553, F557, N658, V659) located near the cytoplasmic ends of the S5 and S6 domains of the hERG subunit [15]. The putative binding site for RPR260243 is distinct from the site described for drugs that block hERG channels. The binding site for structurally diverse blockers was previously localized to specific residues in S6 and the base of the pore helix that face toward the central cavity [33]. F656 and Y652 in S6 are the most important residues for binding of blockers [33,34]. Future studies to identify the interactions of hERG activators with specific residues of the hERG channel and link these interactions with biophysical effects will increase our understanding of hERG channel gating. Such studies will also lead to optimized designs of novel hERG activators (or their avoidance).

In summary, A-935142 increases hERG current by complex mechanisms. Future identification of the binding site(s) for this unique compound will likely provide relevant structural information in understanding the gating mechanisms of the hERG channel, guide in silico efforts to design (or avoid) hERG activators, and contribute to greater safety of non-cardiovascular drugs.

References

[1] Sanguinetti MC, Jiang C, Curran ME, Keating MT. A mechanistic link between an inherited and an acquired cardiac arrhythmia: HERG encodes the Ikr potassium channel. Cell 1995;81:299–307.
[2] Trudeau MC, Warmke JW, Ganetzky B, Robertson GA. HERG, a human inward rectifier in the voltage-gated potassium channel family. Science 1995;269:92–5.
[3] Tseng GN. I(Kr): the hERG channel. J Mol Cell Cardiol 2001;33:835–49.
[4] Keating MT, Sanguinetti MC. Molecular and cellular mechanisms of cardiac arrhythmias. Cell 2001;104:569–80.
[5] Viskin S. Long QT syndromes and torsades de pointes. Lancet 1999;354:1625–33.
[6] Cavero I, Mestre M, Guillon JM, Crumb W. Drugs that prolong QT interval as an unwanted effect: assessing their likelihood of inducing hazardous cardiac dysrhythmias. Exp Opin Pharmacother 2000;1:947–73.
[7] De Ponti F, Poluzzi E, Cavalli A, Recanatini M, Montanaro N. Safety of non-antiarrhythmic drugs that prolong the QT interval or induce Torsade de Pointes. Drug Saf 2002;25:263–86.
[8] Gintant GA, Su Z, Martin RL, Cox BF. Utility of hERG assays as surrogate markers of delayed cardiac repolarization and QT safety. Toxicol Pathol 2006;34:81–90.
[9] Kang J, Chen XL, Wang H, Ji J, Cheng H, Incardona J, et al. Discovery of a small molecule activator of the human ether-a-go-go-related gene (HERG) cardiac K^+ channel. Mol Pharmacol 2005;67:827–36.
[10] Zhou J, Augelli-Szafran CE, Bradley JA, Chen X, Koci BJ, Volgerg WA, et al. Novel potent human-a-go-go-related gene (hERG) potassium channel enhancers and their in vitro antiarrhythmic activity. Mol Pharmacol 2005;68:876–84.
[11] Hansen RS, Diness TG, Christ T, Demnitz J, Ravens U, Olesen SP, et al. Activation of human ether-a-go-go-related gene potassium channels by the diphenylurea 1,3-bis-(2-hydroxy-5-trifluoromethyl-phenyl)-urea (NS1643). Mol Pharmacol 2006;69:266–77.
[12] Casis O, Olesen SP, Sanguinetti MC. Mechanism of action of a novel human ether-a-go-go-related gene channel activator. Mol Pharmacol 2006;69:658–65.
[13] Hansen RS, Diness TG, Wetter E, Ravens U, Olesen SP, Grunnet M. Biophysical characterization of the new human ether-a-go-go-related gene channel opener NS3623 [N-(4-Bromo-2-(1H-tetrazol-5-yl)-phenyl)-N-(3-trifluoromethylphenyl)urea]. Mol Pharmacol 2006;70:1319–29.
[14] Zeng H, Lozinskaya IM, Lin Z, Willette RN, Brooks DP, Xu X. Mallotoxin is a novel human ether-a-go-go-related gene (hERG) potassium channel activator. J Pharmacol Exp Ther 2006;319:957–62.
[15] Perry M, Sachse FB, Sanguinetti MC. Structural basis of action for a human ether-a-go-go-related gene 1 potassium channel activator. PNAS 2007;104:13827–32.
[16] Gordon E, Lozinskaya IM, Lin Z, Semus SF, Blaney FE, Willette RN, et al. 2-[2-(3,4-Dichloro-phenyl)-2,3-dihydro-1H-isoindol-5-ylamino]-nicotinic acid (PD-307243) causes instantaneous current through human ether-ago-go-related gene potassium channels. Mol Pharmacol 2008;73:639–51.
[17] Xu X, Recanatini M, Roberti M, Tseng G. Probing the binding sites and mechanisms of action of two human ether-a-go-go-related gene channel activators, 1,3-bis-(2-Hydroxy-5-trifluoromethyl-phenyl)-urea (NS1643) and 2-[2-(3,4-dichloro-phenyl)-2,3-dihydro-1H-isoindol-5-ylamino]-nicotinic acid (PD-307243). Mol Pharmacol 2008;73:1709–21.
[18] Zhou Z, Gong Q, Ye B, Fan Z, Makielski JC, Robertson GA, et al. Properties of hERG channels stably expressed in HEK-293 cells studied at physiological temperature. Biophys J 1998;74:230–41.
[19] Su Z, Chen J, Martin RL, McDermott JS, Cox BF, Gopalakrishna M, et al. Block of hERG channel by ziprasidone: biophysical properties and molecular determinants. Biochem Pharmacol 2006;71:278–86.
[20] Gintant GA, Limberis J, McDermott J, Wegner C, Cox BF. The canine Purkinje fiber: an in vitro model system for acquired long QT syndrome and drug-induced arrhythmogenesis. J Cardiovas Pharmacol 2001;37:607–18.
[21] Kamiya K, Mitcheson JS, Yasui K, Kodama I, Sanguinetti MC. Open channel block of HERG K^+ channels by vesnarinone. Mol Pharmacol 2001;60:244–53.
[22] Su Z, Martin RL, Cox BF, Gintant GA. Mesoridazine: an open-channel blocker of human ether-a-go-go-related gene K^+ channel. J Mol Cell Cardiol 2004;36:151–60.
[23] Smith PL, Baukrowitz T, Yellen G. The inward rectification mechanism of the HERG cardiac potassium channel. Nature (Lond) 1996;379:833–6.
[24] Spector PS, Curran ME, Zou A, Keating MT, Sanguinetti MC. Fast inactivation causes rectification of the IKr channel. J Gen Physiol 1996;107:611–9.
[25] Hua F, Johns DC, Gilmour Jr RF. Suppression of electrical alternans by overexpression of HERG in canine ventricular myocytes. Am J Physiol 2004;286:H2342–51.

[26] Royer A, Demolombe S, El HA, Le QK, Piron J, Toumaniantz G, et al. Expression of human ERG K+ channels in the mouse heart exerts anti-arrhythmic activity. Cardiovasc Res 2005;65:128–37.
[27] Killeen MJ, Thomas G, Olsen SP, Demintz J, Stokoe KS, Grace AA, et al. Effects of potassium channel openers in the isolated perfused hypokalaemic murine hearts. Acta Physiol 2008;193:25–36.
[28] Brugada R, Hong K, Cordeiro JM, Dumaine R. Short QT syndrome. CMAJ 2005;173:1349–53.
[29] Bjerregaard P, Jahangir A, Gussak I. Targeted therapy for short QT syndrome. Expert Opin Ther Targets 2006;10:393–9.
[30] Dobrev D, Ravens U. Remodeling of cardiomyocyte ion channels in human atrial fibrillation. Basic Res Cardiol 2003;98:137–48.
[31] Itoh H, Horie M, Ito M, Imoto K. Arrhythmogenesis in the short-QT syndrome associated with combined hERG channel gating defects—a simulation study. Circ J 2006;70:502–8.
[32] Cordeiro JM, Brugada R, Wu YS, Hong K, Dumaine R. Modulation of IKr inactivation by mutation N588K in KCNH2: a link to arrhythmogenesis in short QT syndrome. Cardiovas Res 2005;67:498–509.
[33] Mitcheson JS, Chen J, Lin M, Culberson C, Sanguinetti MC. A structural basis for drug-induced long QT syndrome. Proc Natl Acad Sci USA 2000;97:12329–33.
[34] Mitcheson JS, Perry M, Stansfeld P, Sanguinetti MC, Witchel H, Hancox J. Structural determinants for high-affinity block of hERG potassium channels. Novartis Found Symp 2005;266:136–50.